

Clastic record from Northern Tethyan Himalaya: Implication for the initial India-Asian collision in the western Yarlung-Zangpo suture zone, South Tibet[☆]

Xu-dong Guo^a, Lin Ding^{b,d}, Fu-long Cai^{b,d}, Gui-zhen Guo^a, Xiao-yan Xu^{b,d}, Peng Han^a, Chang-jun Gu^a, Mei-yu Liu^a, Xiang-li Ding^c, Xu Liu^a, Xin-lei Li^a, Deng Zeng^b, Ya-hui Yue^b, Qiu-yun Guan^{c,*}

^a National Disaster Reduction Center of China, Beijing 100124, China

^b State Key Laboratory of Tibetan Plateau Earth System, Resources and Environment (TPESRE), Institute of Tibetan Plateau Research, Chinese Academy of Sciences, Beijing 100101, China

^c Chinese Academy of Geological Sciences, Beijing 100037, China

^d University of Chinese Academy of Sciences, Beijing 100049, China

ARTICLE INFO

Editor: Prof. S Shen

Keywords:

Cenozoic foreland basin
Detrital zircon U-Pb
India-Asia collision
Yarlung-Zangpo suture zone

ABSTRACT

The suturing process between the Indian and Asian continents in the western part of the Yarlung-Zangpo Suture Zone (YZSZ) remains unclear due to the challenging environment and the complex geological background. The bilateral material of two continents provides robust evidence for constraining the timing of the continental collision. In this study, we conducted field mapping, geochronology and provenance analyses on sandstones from the Weimei, Rilang and Denggang formations (Upper Jurassic to Eocene) within a same section in the Zhongba area. The Weimei and Rilang formations exhibit typical characteristics of Tethyan Himalayan provenance, recording the evolution of the northern margin of the Indian continent during Late Jurassic - Cretaceous. The Paleocene - Eocene Denggang formation displays a provenance distinct from the Tethyan Himalayan strata, closely aligning with the Asian deposits in the YZSZ. In the Tethyan Himalaya area, the appearance of Asian debris in the Denggang formation indicates that the collision between India and Eurasia had occurred. The maximum depositional ages of the sandstones from the Denggang formation constrain the collision between the Indian and Asian continents in the western YZSZ to no later than 56 Ma - 54 Ma.

1. Introduction

The Yarlung-Zangpo Suture Zone (YZSZ) contains critical evidence regarding the subduction of the Neo-Tethys Ocean and the collision between the Indian and Eurasian plates (Yin and Harrison, 2000; Kapp and DeCelles, 2019). Furthermore, the India-Asia collision drove the deep processes that shaped the unique Himalayan-Tibetan Plateau orogenic belt and profoundly influenced the interactions and coupling among various surface spheres (Ding et al., 2022). However, the precise timing of the initial India-Asia collision and subsequent suturing processes remain controversial (Ding et al., 2005; Aitchison et al., 2007; Van Hinsbergen et al., 2012; Yuan et al., 2021). Multi-stage subduction systems of the Neo-Tethys Ocean have been identified in the Myanmar

(eastern YZSZ) and the Kohistan-Ladakh region (western YZSZ) (Buckman et al., 2018; Yang et al., 2022). Nonetheless, in the central-eastern YZSZ, only the single-stage model has sufficient evidence (Ding et al., 2005; Cai et al., 2011, 2012; Hu et al., 2015; Wei et al., 2020a, 2020b; An et al., 2021; Guo et al., 2022). Concerning the timing of initial collision, different definitions and methods exhibit substantial discrepancies (Ding et al., 2017, and references therein). Both peripheral foreland basin analysis and paleomagnetic studies have been demonstrated as effective approaches for constraining the timing of initial collision (Ding et al., 2017). Even so, there is still controversy over the recent high-quality paleomagnetic data applied to the reconstruction of Greater India, resulting in significant discrepancies in initial collision time and closure patterns (Meng et al., 2023; Yuan et al., 2023). By

[☆] This article is part of a Special issue entitled: 'Tethyan Tectonic Domain' published in Palaeogeography, Palaeoclimatology, Palaeoecology.

* Corresponding author.

E-mail address: guanqiyun@itpcas.ac.cn (Q.-y. Guan).

contrast, the method of peripheral foreland basin integrates a comprehensive geological chain including sedimentology, structural deformation, and provenance analysis, constraining the initial collision to 65–55 Ma (Fig. 1) in the central-eastern YZSZ (Ding et al., 2017; Wei et al., 2020a, 2020b). Among these approaches, provenance analysis has proven particularly effective in constraining the age of continental collision (Ding et al., 2005; Wang et al., 2011; Hu et al., 2015; An et al., 2021).

The YZSZ in the western segment exhibits notable tectonic differences and can be structurally subdivided into two subzones that encircle the Zhongba microcontinent/block (abbreviated as Zhongba unit), which is a Sinian/Ordovician-Triassic meta-sedimentary unit. A contentious issue has arisen concerning the classification of these metamorphic strata, with debate centered on whether they constitute an independent geological unit or are merely a component of the Indian plate (Gansser, 1983; Li et al., 2014; Cheng et al., 2024; Zhou et al., 2025). Owing to limited research data, the tectonic evolution of the western YZSZ and the relationships between its constituent units remain poorly constrained. The key to addressing this issue lies in conducting research on the evolutionary history of different units and determining the timing of major events.

In this study, we present new findings from a northern Tethyan Himalaya sequence through detailed structural and stratigraphic analysis of quartz sandstone, volcaniclastic sandstone, chert, and limestone in the Naju area, southwestern Zhongba district. Four sandstone samples were collected from the studied section to constrain the first occurrence of Asian provenance in northern Tethyan Himalayan strata. Combining field and geochronological data, we establish an updated stratigraphic framework with paleoenvironmental and provenance interpretations for the northern Tethyan Himalaya in western YZSZ. Furthermore, we propose that the first appearance of Lhasa-derived detrital zircons (marking the initial India-Asia collision) in this area occurred no later than the early Eocene.

2. Geological background

Our study area is located in the Zhongba area of southern Tibet and comprises the Lhasa terrane, the YZSZ, and Tethyan Himalaya sequences from north to south (Fig. 1).

The Lhasa terrane can be further subdivided into the north Lhasa, central Lhasa, and south Lhasa terranes, primarily bounded by the Shiquanhe - Nam Tso mélange zone and the Luobadui-Milashan Fault (Zhu et al., 2011a). The Gangdese arc is located along the southern margin of the south Lhasa terrane, which constituted the southernmost edge of the Asian continent prior to the India-Asia collision (Wang et al., 2016,

2017a; Zhu et al., 2018). As the product of Neo-Tethyan subduction and the subsequent India-Asia collision, the Gangdese arc preserves a continuous magmatic record from the Middle Triassic to the Miocene (Zhu et al., 2011a, 2011b; Zhang et al., 2014; Wang et al., 2016). However, the spatial distribution of the magmatic rocks with different ages exhibits significant variations (Zhu et al., 2018). For example, Late Cretaceous magmatic rocks are primarily concentrated in the Gangdese arc region east of the Lazi area (Guo et al., 2024). In the entire Gangdese area, the latest Cretaceous to Eocene Linzizong group (a volcanic-sedimentary sequence) is widely distributed and can be divided into the Dianzhong, Nianbo, and Pana formations from bottom to top (Chen et al., 2016). The Dianzhong formation, triggered by the Neo-Tethyan slab rollback, records the late stage of Neo-Tethyan subduction (Zhu et al., 2015; Jiang et al., 2018). The Nianbo formation, which consists of rhyolites interbedded with fluvial sandstone, conglomerate, and tuff, represents the tectonic transition from the ongoing collision to Neo-Tethyan slab break-off (Zhu et al., 2015). The magmatic rocks of the Pana formation reveal significant crustal thickening associated with the final stage of Neo-Tethyan break-off (Zhu et al., 2015).

In the western YZSZ, the suture zone can be further subdivided into the northern subzone, the Zhongba unit, and the southern subzone (Fig. 2). The northern subzone encompasses the Xigaze forearc basin, the ophiolitic complex, and the sedimentary mélange (Orme et al., 2015; Liu et al., 2018; Cui et al., 2021). On the north side, the northern subzone and the Gangdese batholith are separated by the Great Counter Thrust, which is typically overlain by the Miocene Dazhuka conglomerate (Kailas conglomerate) (Murphy and Yin, 2003; Laskowski et al., 2017). In the eastern part of this segment, the Xigaze forearc basin displays the Cenozoic Tso-jiangding group, which represents wedge-top deposits within its hanging wall (Ding et al., 2005; Orme et al., 2015; Hu et al., 2016). Comparable sedimentary units include the Dajin Formation near the Kailas region and the Dajiweng Formation to the west, though their tectonic affinities remain unresolved and demand further systematic investigation (Wang et al., 2015; Li et al., 2016; Sun et al., 2018). The ophiolitic and sedimentary mélange comprise Permian limestone blocks, Middle-Lower Triassic seamounts, Jurassic bedded cherts, and Early Cretaceous intermediate-basic rocks, representing the evolution of either a small oceanic basin or the Neo-Tethys Ocean during the Mesozoic (Zhang et al., 2005; Cui et al., 2021; Liu et al., 2021; Zhou et al., 2025).

The Zhongba unit, situated between the northern and southern subzones, are composed of a series of Paleozoic to Early Mesozoic metamorphic sedimentary strata and Early Triassic volcanic rocks (Sun and Hu, 2012; Li et al., 2023a; He et al., 2024). Li et al. (2023a) reports Late Neoproterozoic biotite-plagioclase gneiss near Gongzhu Co, which

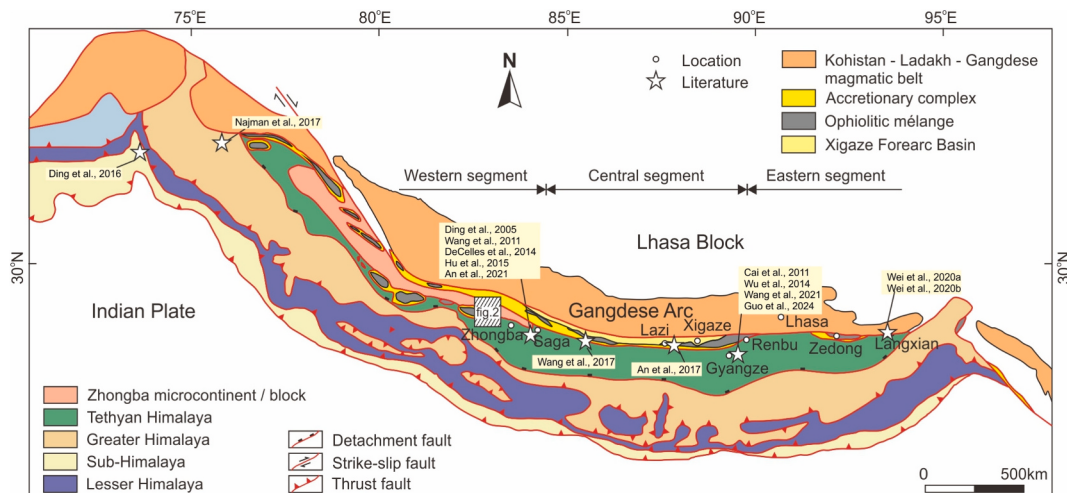


Fig. 1. Geological map of the YZSZ with provenance analysis literature from different locations (modified after Liu et al., 2018).

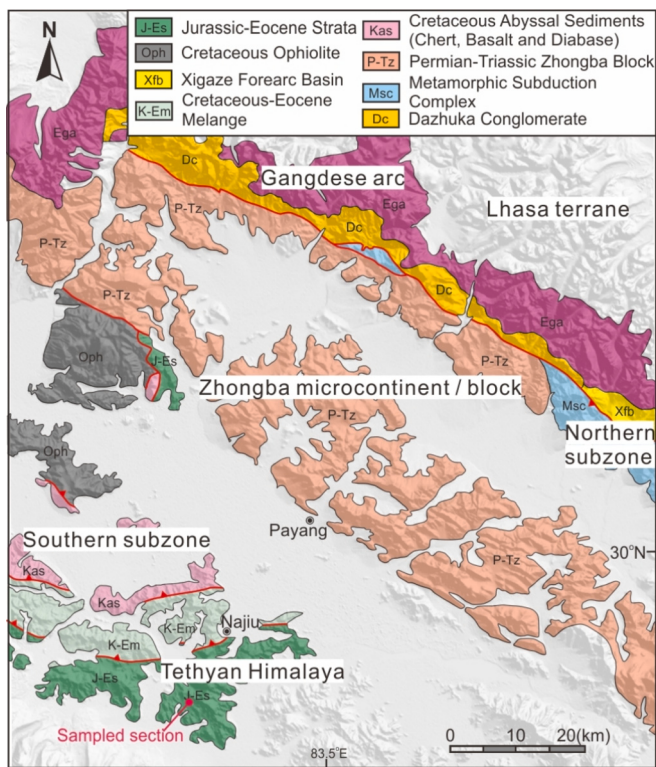


Fig. 2. Geological map of the study area (modified after Hebei Institute of Geological Survey, 2006).

represents the continental basement of the Zhongba unit. Paleomagnetic data and provenance analyses confirm that this stratigraphic unit constitutes an extension of Greater India prior to the Late Paleozoic (Sun and Hu, 2012; Li et al., 2024). However, studies on warm-water fauna occurrences suggest that the Zhongba unit may have rifted from the Indian plate prior to the late Cisuralian (Cheng et al., 2022). Recently, Cheng et al. (2024) mentioned unpublished arc-associated magma records in the Zhongba unit, which further supports their evolution as an independent terrane.

The southern subzone consists of Early Cretaceous ophiolite rocks, Middle Jurassic to Late Cretaceous pelagic sediments, and Late Cretaceous subduction complex. The ophiolitic data reveal complicated processes of oceanic plate expansion, subduction, and plume influence (Dai et al., 2012; Cheng et al., 2018; Xiong et al., 2020). Wei et al. (2015) subdivided the southern subzone into five distinct units and proposed its origin as a remnant oceanic basin developed south of the Zhongba unit. Provenance analyses of Late Cretaceous sandstone blocks within the Naju mélange demonstrate a genetic linkage between the southern subzone and the Lhasa terrane (Guo et al., 2019). Part of the nappe is thrust over the Eocene mélange, indicating that the south-directed imbricate thrusting must postdate the initial collision (Xu et al., 2015).

The Tethyan Himalaya sequence is commonly believed to represent the northern margin of the Indian plate and is divided into northern and southern parts based on the Gyrong-Kangmar thrust (Antolín, 2010). In the western part of the YZSZ, the study area are exposed in a narrow area between the Greater Himalaya and the southern subzone of the YZSZ (Fig. 1). Four formations have been identified, which reflect a passive continental evolution from Jurassic to Late Cretaceous (Du et al., 2015). These strata correlate well with those exposed in the Gyangze region, representing the northern Tethyan Himalayan domain (Du et al., 2015; Jin et al., 2024).

3. Strata and sampling

The study section is located south of Naju Village, forming part of the northern Tethyan Himalayan sequence (Fig. 2). The strata in the study area are generally subjected to fold deformation, with axial traces trending approximately east-west. The formations investigated here are part of a Jurassic to Eocene sequence, composed of the Weimei formation, the Rilang formation, the Duobeng formation (also known as Gyabula formation), the Chuangde formation, and the Denggang formation (Du et al., 2015; Fig. 3). The Weimei formation is predominantly composed of thick-bedded quartz sandstone, with minor occurrences of ripple marks observed (Du et al., 2015; Figs. 3a). In the study area, contemporaneous diabase dikes associated with the Rilang formation are commonly intrude into the Weimei formation (Wei et al., 2017). The Rilang formation conformably overlies the Weimei formation. It is primarily composed of yellow-green volcaniclastic sandstone interbedded with shale and mudstone, and the surface of sandstone beds often exhibits spherical weathering (Zhang et al., 2015, Figs. 3b). Furthermore, the Rilang formation is characterized by a northward paleocurrent direction and is usually interpreted as a deep-sea submarine fan deposit linked to the breakup of the Indian plate (Zhang et al., 2015). The Duobeng formation consists of thin-bedded chert interbedded with siliceous mudstone and occasional sandstone layers (Figs. 3c). The Duobeng formation can be correlated well with the Gyabula formation in the Tethyan Himalaya, located in the central part of the YZSZ. The Chuangde formation is characterized by red-bedded limestone and blocks (Figs. 3d). In the study area, the Chuangde formation conformably overlies the Duobeng formation (Du et al., 2015), but it is only locally exposed within the studied section. Due to limited exposure, it was difficult to determine whether the contact between the Denggang and Chuangde formations is tectonic or depositional. In the central and western regions of the YZSZ, the Denggang formation (synonymous with the Sangdanlin formation) overlies the red limestone (Chuangde formation) of the northern Tethyan Himalayan. It shows an upward transition from chert and siliceous mudstone to sandstone-dominated clastic rocks. In the study section, the Denggang formation is composed of siliceous mudstone, layered siltstone, and exotic blocks of sandstone and chert (Figs. 3e, f). Additionally, previous studies have reported Seladian–early Thanetian radiolarian assemblages in both the studied section and adjacent sections (Liang et al., 2012; Li et al., 2018; Cheng et al., 2024). In this study, we sampled four sandstone from the Weimei formation (2020Tzb18), the Rilang formation (2020Tzb11) and the Denggang formation (2021Tzb04, 2021Tzb05) within the same section from the Tethyan Himalaya. The stratigraphic architecture is illustrated in Fig. 3g.

4. Methods

Petrographic analyses were performed on all samples, with more than 300 grains counted for each (Dickinson, 1985). The four sandstone samples (2020Tzb11, 2020Tzb18, 2021Tzb04, 2021Tzb05) were analyzed for detrital zircon U–Pb dating using LA-ICP-MS at the State Key Laboratory of Tibetan Plateau Earth System, Resources and Environment, Institute of Tibetan Plateau Research, Chinese Academy of Sciences (ITPCAS). For each sample, zircon grains were randomly selected throughout the entire process, from pre-treatment to dating. The internal structure of the zircon grains was analyzed using a Gatan MiniCL cathodoluminescence (CL) spectrometer equipped on a JEOL JSM-IT300 scanning electron microscope. Each sandstone selected 100 zircon grains, choosing the clear parts for dating. In this study, the weighted mean ages of 91500 and GJ-1 are 1046.7 ± 3.3 Ma (MSWD = 2.1, $n = 33$) and 600.89 ± 0.61 Ma (MSWD = 1.2, $n = 41$), respectively, which are consistent with the established values (91,500: 1065.4 ± 0.3 Ma, Wiedenbeck et al., 1995; GJ-1: 599.8 ± 4.5 Ma, Jackson et al., 2004). Four kinds of methods were prepared to constrain the sedimentary age of strata: the youngest single detrital zircon (YSG); the youngest

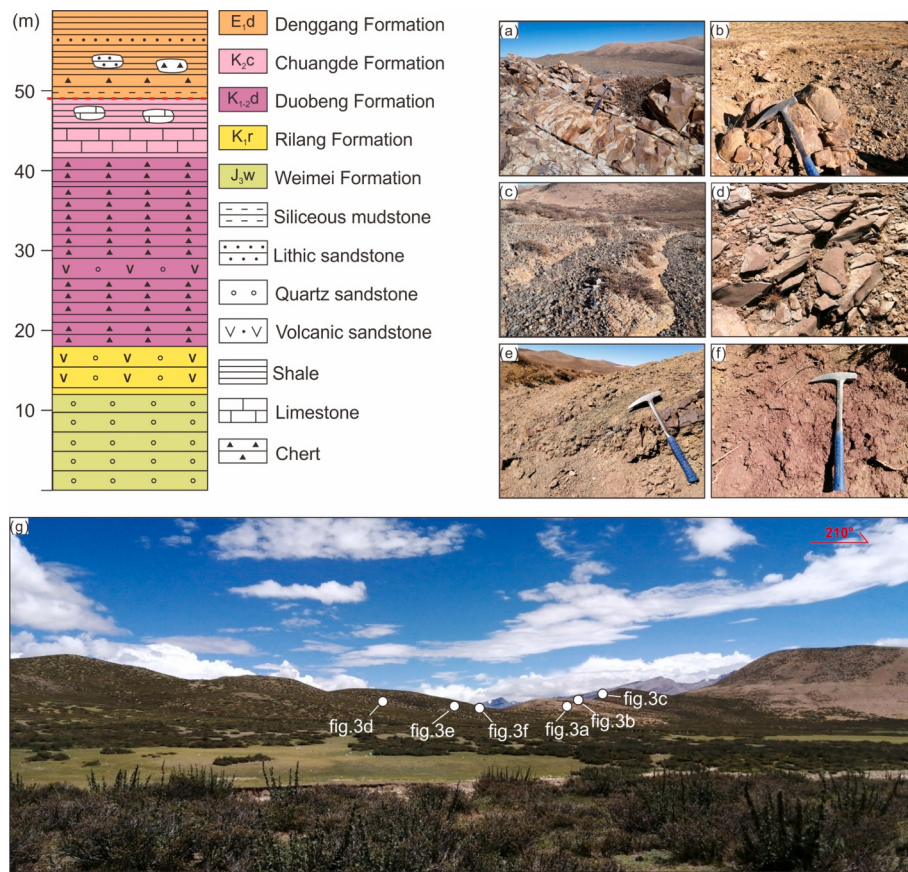


Fig. 3. Stratigraphic column of the Tethyan Himalaya in the study area (modified after Liang et al., 2012; Du et al., 2015; Li et al., 2018). a. Pure quartz sandstone in the Weimeい formation; b. Spherically weathered lithic sandstone in the Rilang formation; c. Layered cherts in the Duobeng formation; d. Limestone of the Chuande formation; e. Mudstone and interbedded siltstone of the Denggang formation; f. Siliceous mudstone in the Denggang formation; g: the stratigraphic section in this study.

graphical detrital zircon age peak on an age probability plot (YPP); the weighted mean age ($\pm 1\sigma$, which includes both internal analytical error and external systematic error) of the youngest cluster of two or more grain ages ($2 \leq n \leq 13$) that overlap in age at 1σ [YC1 σ (2+)]; and the weighted mean age ($\pm 1\sigma$, incorporating both internal analytical error and external systematic error) of the youngest cluster of three or more grain ages ($3 \leq n \leq 24$) overlapping in age at 2σ [YC1 σ (3+)]. The depositional age of the strata was determined using the YC1 σ (2+) method based on the maximum depositional ages (MDAs) from Dickinson and Gehrels (2009).

Machine learning (ML) is a robust and efficient technique that can automatically learn from experience to recognize complex patterns and relationships in data. In contrast to traditional classification approaches, such as geochemical plotting, ML enables autonomous identification of classification features without relying on pre-existing knowledge. By leveraging algorithms, ML can uncover intricate relationships within the data, thereby achieving superior classification accuracy. Zhong et al. (2023) trained three machine learning models, namely, Support Vector Machine (SVM), Random Forest (RF), and Multilayer Perceptron (MLP), using published and well-established magmatic zircon data to distinguish the magmatic origin of zircons. Here, we employ the three machine learning models trained by Zhong et al. (2023) to discuss the magmatic origin of detrital zircons. To screen out magmatic zircons and exclude the influence of inclusions, we applied stricter selection criteria than those in the original text. The magmatic zircons must meet the criteria of $\text{La} < 1 \text{ ppm}$, $\text{Th}/\text{U} > 0.2$, and $\text{U}/\text{Ce} < 100$ (Grimes et al., 2015; Zhong et al., 2023). Furthermore, to minimize the impact of model errors, results were retained only when the classification results of the three models are consistent.

5. Result

5.1. Sandstone petrology

Although the samples (2021Tzb04, 2021Tzb05) from the Denggang formation are siltstones and fine-grained sandstone, we still counted them to extract their sedimentary information. Sample 2021Tzb04 is composed of 40 % quartz, 23 % feldspar, and 37 % lithic fragments (Figs. 4a, 5). Among these, the quartz is predominantly monocrystalline quartz (comprising 37 %), volcanic lithic fragments make up 6 %, sedimentary fragments account for 18 % (rich in siliceous lithic fragments), and metamorphic fragments account for 13 %. Sample 2021Tzb05 comprises 50 % quartz, 23 % feldspar, and 27 % lithic fragments (Figs. 4b, 5). The quartz predominantly consists of monocrystalline quartz (46 %). Volcanic lithic fragments constitute 5 %, sedimentary fragments (with a high content of siliceous fragments) 17 %, and metamorphic fragments 5 %. The sample (2020Tzb11) from the Rilang formation is composed of 63 % quartz, of which 57 % is monocrystalline quartz, 22 % feldspar, and 15 % lithic fragments, including 10 % volcanic fragments (Figs. 4c, 5). The sample (2020Tzb18) from the Weimeい formation exhibits an extremely high monocrystalline quartz content (94 %), along with small percentages of polycrystalline quartz (1 %), feldspar (2 %), and lithic fragments (3 %) (Figs. 4d, 5).

5.2. Detrital zircon U—Pb results

The MDAs of sandstone samples are summarized in Table 1, and all the normalized probability plots of the sandstones are shown in Fig. S1. Samples from the Denggang formation (2021Tzb04 and 2021Tzb05)

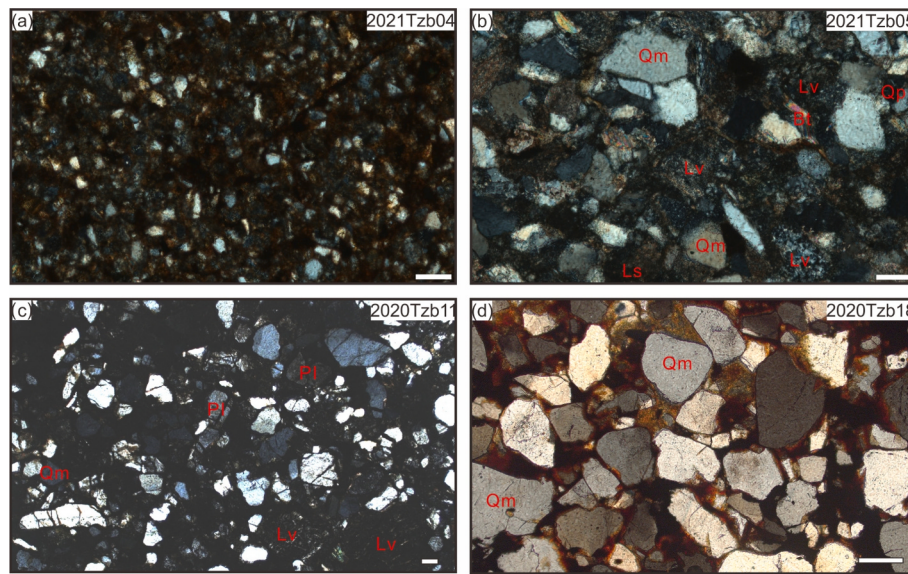


Fig. 4. Petrofacies of the Denggang, Rilang and Weimei formations. All scale bars = 100 μm . a–b: Sandstone from the Denggang formation; c: Sandstone from the Rilang formation; d: Sandstone from the Weimei formation. Bt: biotite; Pl: plagioclase; Ls: sedimentary lithics; Lv: volcanic lithics; Qm: monocrystalline quartz; Qp: polycrystalline quartz.

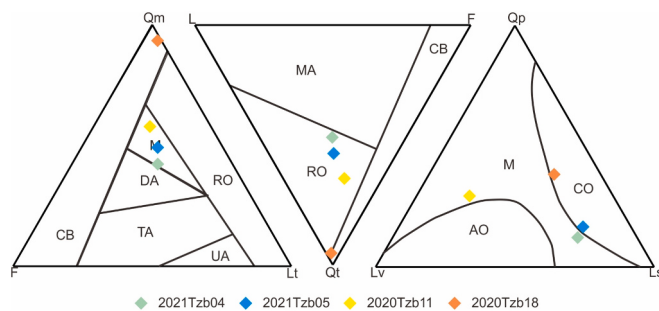


Fig. 5. Detrital modes of the sandstones from the Denggang, Weimei and Rilang formations in the Zhongba area. Abbreviations: RO: recycled orogen; CB: continental block; MA: magmatic arc; DA: dissected arc; TA: transitional arc; UA: undissected arc; CO: collisional orogen; AO: arc orogen; F: feldspar; L: lithic; Lt: total lithics; Qt: total quartz.

exhibit similar geochronological features, with Cenozoic peaks ranging from 63 Ma to 56 Ma. In the Mesozoic, zircon ages dominated in Cretaceous with the highest peaks at 91 Ma to 88 Ma and subordinate peaks at 129 Ma to 127 Ma. Pre-Mesozoic ages, representing a minor fraction, range from 3362 Ma to 314 Ma, with no distinct clusters (Fig. S1). Sample (2020Tzb11) from the Rilang formation shows a single peak at 130 Ma in the Mesozoic. The pre-Mesozoic ages are characterized by a strong peak at 537 Ma, with subordinate peaks at 2461 Ma, 980 Ma, 925 Ma, 618 Ma (Fig. S1). The Weimei formation (2020Tzb18) lacks Mesozoic grains. Most of the grains in Weimei formation are clustered around 1162 Ma to 792 Ma, 679 Ma to 614 Ma and 546 Ma to 492 Ma, with the highest peak at ~542 Ma and other peaks at 1158 Ma, 642 Ma (Fig. S1).

Table 1

Summary of the characteristics of detrital zircon U–Pb ages of samples in the Denggang, Weimei and Rilang formations.

Sample	Outcrop	YSG/Ma	YPP/Ma	YC1 σ (2+)/Ma	MSWD	YC2 σ (3+)/Ma	MSWD
2021Tzb04	Denggang formation	56 ± 2	63	56.6 ± 2.6	0.069, n = 3	60 ± 2.9	2.7, n = 5
2021Tzb05	Denggang formation	50 ± 2	56	53.8 ± 1.2	0.055, n = 2	54.6 ± 1.5	1.9, n = 7
2020Tzb11	Rilang formation	128 ± 1	130	129.4 ± 1	0.71, n = 6	129.4 ± 1	0.71, n = 6
2020Tzb18	Weimei formation	410 ± 3	523	493.4 ± 4.2	0.32, n = 3	496 ± 3.4	1.18, n = 5

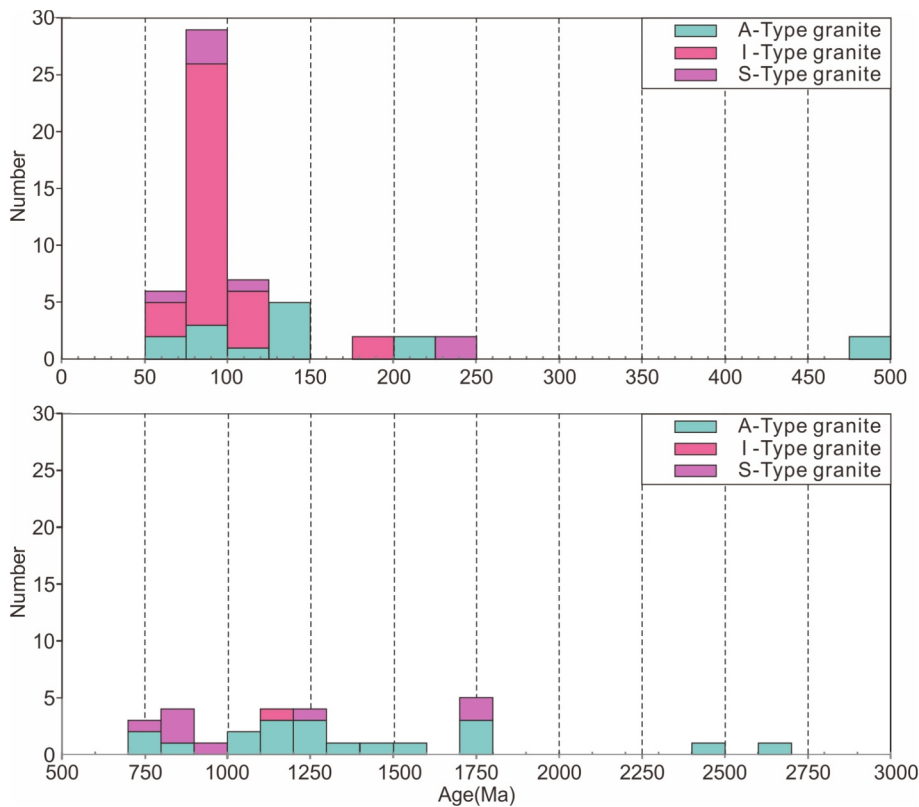


Fig. 6. The source classification results of magmatic detrital zircons from the Denggang formation using machine learning classifiers.

Strata in the Paleocene foreland basin and the Paleocene-Eocene Xigaze forearc basin (Tso-jiangding group) commonly show a youngest peak at ~56 Ma, with the highest peak around ~90 Ma, similar to the magmatic rocks in Gangdese arc (Fig. 7; Cai et al., 2012; Hu et al., 2015). The accretionary wedge in the central YSZS, which records the history of subduction and accretion along the southern margin of the Lhasa terrane during the Cretaceous (related to Neo-Tethyan subduction), exhibits a consistent highest peak matching the Gangdese arc at ~90 Ma (Fig. 7; Ziaibrev et al., 2004; Guo et al., 2022). In the pre-Mesozoic period, the accretionary wedge exhibits its highest peak at 1170 Ma, 980 Ma - 940 Ma, and 580 Ma - 520 Ma. Furthermore, the peak of 1170 Ma is a significant signature of the Lhasa terrane, providing evidence for the Lhasa terrane origin from Australia (Zhu et al., 2011a, 2011b). The clastic rocks of Naju mélange in western YSZS also show characteristics of the Lhasa terrane provenance (Fig. 7; Guo et al., 2019). Unlike the accretionary wedge in central YSZS, the Naju mélange lacks a peak at 130 Ma, with the highest peak age occurring at 89 Ma (Guo et al., 2019). The Tethyan Himalaya is generally considered the northernmost edge of the Indian plate. As part of the passive continental margin, magmatic activity in the Tethyan Himalaya is limited, with only a magmatic event at 130 Ma linked to India-Australia rifting (Hu et al., 2010; Du et al., 2015). The Cretaceous Tethyan Himalaya has peak at 130 Ma, corresponding to the volcanic age of the Wolong formation (Fig. 7; Hu et al., 2010). The pre-Cretaceous Tethyan Himalaya strata lack Mesozoic zircons, but show the pre-Mesozoic peaks at 950 Ma and 530 Ma (Cai et al., 2016).

6.1.2. Interpretations of detrital zircon provenance

The Weimei and Rilang formations exhibit the highest pre-Mesozoic peak at ~542 Ma to 536 Ma and lack the typical features of the Lhasa terrane, most closely resembling the Tethyan Himalaya strata (Fig. 7). The Rilang formation, characterized by a single Cretaceous peak in the Mesozoic, is also consistent with the Cretaceous Tethyan Himalayan strata (Fig. 7). In the Denggang formation, zircons are concentrated within the period of 150 Ma to 50 Ma, corresponding well with the

subduction history of the Neo-Tethys oceanic crust along the southern margin of the Lhasa terrane (Zhu et al., 2015; Wang et al., 2017a). The youngest peak (~56 Ma) and the highest peak (~88 Ma) ages in the Denggang formation are commonly observed along the southern Asian continental margin, with the highest peak age being comparable to the early Late Cretaceous 'flare-up' events in the eastern Gangdese arc (Fig. 7). Moreover, the percentage of I-Type granitic zircon is also consistent with published data from the eastern Gangdese arc (Fig. 6; Ji et al., 2009; Ma et al., 2022). Therefore, the provenance of the Denggang formation is derived from the Lhasa terrane. Furtherly, combined with the westward younging trend of the Xigaze forearc basin since the Late Cretaceous and the east-to-west distribution of trench-related sediments from the Ancestral Lhasa River, the eastern Gangdese arc is a major provenance for the Denggang Formation (Wu et al., 2010; Orme et al., 2021).

6.2. Stratigraphic chronology

The Weimei formation shows significant differences between the ages of YSG and YC1σ(2+). Thus, the MDAs cannot reliably constrain the true depositional age of the Weimei formation (Table 1). In Gyangze area, ammonites and magmatic zircons constrain the terminal age of the Weimei Formation at the Jurassic/Cretaceous boundary (Liu et al., 2013; Li et al., 2020a). In the Naju area, radiolarian assemblages from chert-siliceous mudstone interlayers in the Weimei formation provide a depositional age at middle Tithonian (Cheng et al., 2024). Diabase dikes (129.8 ± 1.3 Ma) intruding into the Weimei formation also indicate that the upper part of the Weimei formation cannot be younger than the early Hauterivian age (Wei et al., 2017). Based on integrated MDAs and the depositional age of the Duobeng formation, the Rilang formation can be well constrained to the early Aptian (Fig. 8; 2004; Li et al., 2018; Cheng et al., 2024). Previous researchers in the Zhongba area sampled radiolarian assemblages from the Duobeng formation and dated them to the latest Barremian–Cenomanian interval (Li et al., 2020b, 2023b; Cheng

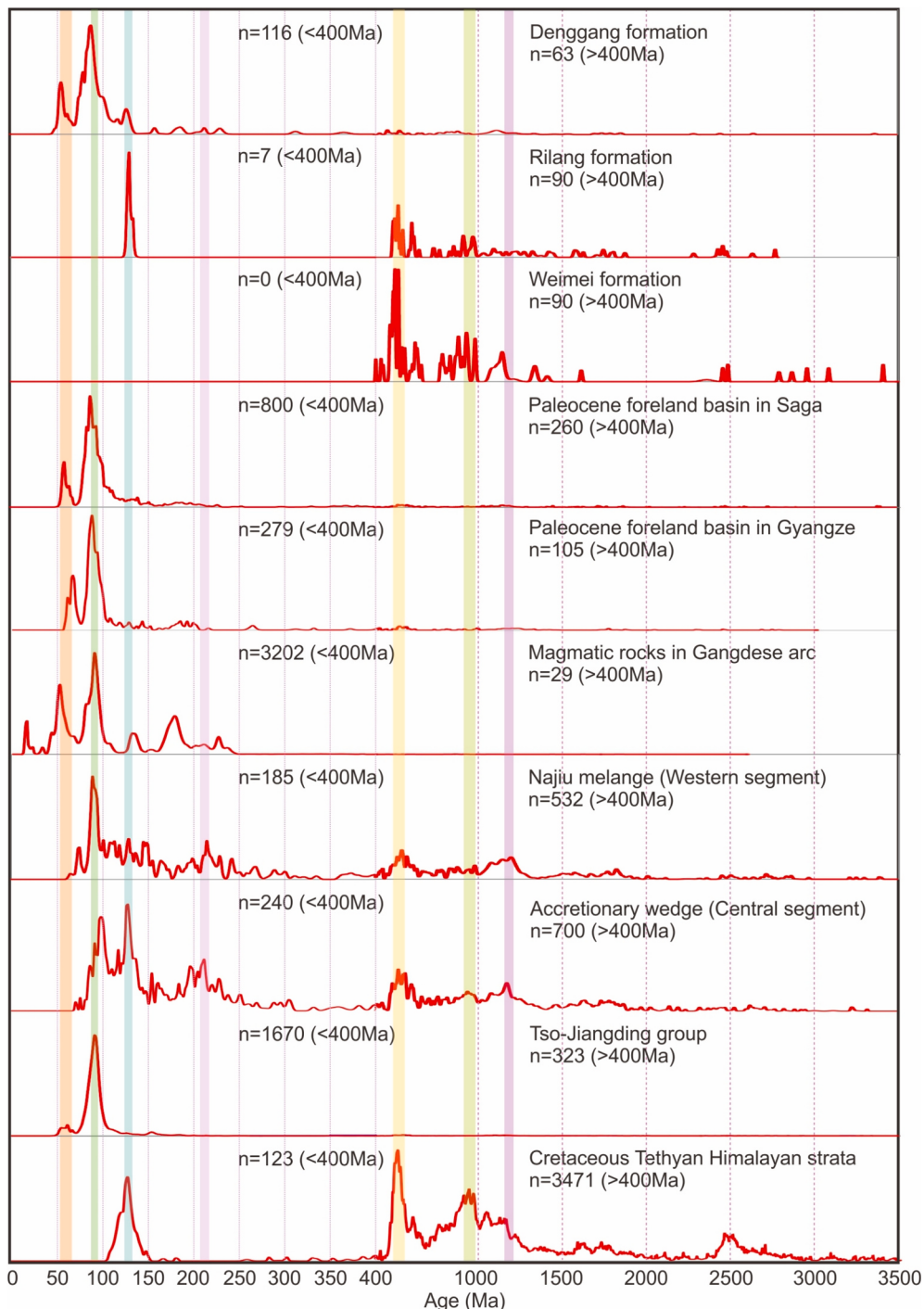


Fig. 7. Normalized probability plots in this study and related geological units. Paleocene foreland basin in Saga (DeCelles et al., 2014; Hu et al., 2015; Wang et al., 2017b; An et al., 2021); Paleocene foreland basin in Gyangze (Wu et al., 2014; Guo et al., 2024); Magmatic rocks in the Gangdese arc (Guo et al., 2022 and references therein); The Naju mélange (Guo et al., 2019); Accretionary wedge in central YZSZ (Cai et al., 2012; An et al., 2017; Guo et al., 2022); The Tso-jiangding group of Xigaze forearc basin (Ding et al., 2005; Orme et al., 2015; Hu et al., 2016); The Cretaceous Tethyan Himalaya (Wang et al., 2017b and references therein).

et al., 2024). The Upper Cretaceous oceanic red beds of the Chuangde formation are stratigraphically correlated across southern Tibet, but no chronological data are available for the Zhongba area. In the Gyangze and Kangmar areas, benthic and planktic foraminifers from the Chuangde formation are dated to the middle to late Campanian, with some local occurrences extending into the early Maastrichtian (ca. 70 Ma; Chen et al., 2011; Li et al., 2011; Fang et al., 2020). Samples from the Denggang formation have $YC1\sigma(2+)$ at 56 Ma - 54 Ma sourcing from Lhasa terrane (Gangdese arc). During the Paleocene to Eocene, the

Gangdese area has continuously outcropped volcanic records (the Linzizong group), indicating that the MDAs of sandstone samples can be reasonably constrained by the $YC1\sigma(2+)$ ages (Dickinson and Gehrels, 2009). Considering the presence of Thanetian radiolarian assemblages in the lower siliceous mudstone, the Denggang formation is dated to the late Paleocene to early Eocene (Fig. 8; Liang et al., 2012; Li et al., 2018; Cheng et al., 2024).

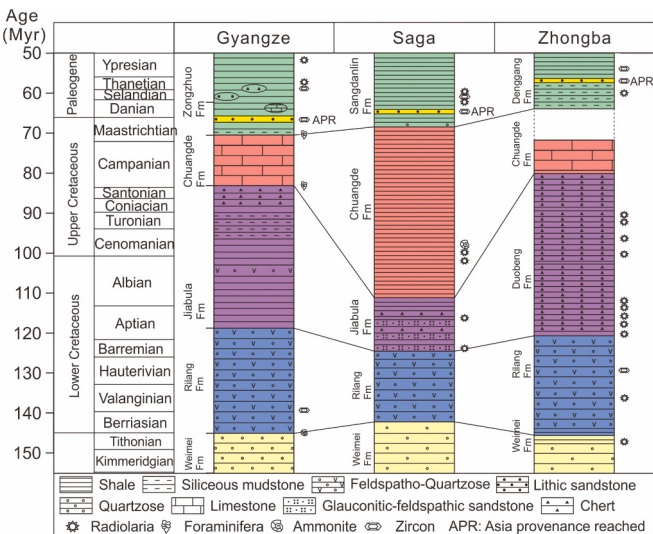


Fig. 8. Simplified stratigraphy of the Upper Jurassic to Eocene stratigraphic units in the Tethyan Himalaya. The Gyangze area after (Liu et al., 2013; Li et al., 2020a; Colpaert and Li, 2021; Wang et al., 2021; Guo et al., 2024); The Saga area after (An et al., 2021; Li et al., 2023c); The Babazhadong section in the Zhongba area (study area) after (Du et al., 2015; Li et al., 2023b; Cheng et al., 2024).

6.3. Initial collision of India-Asia and tectonic evolution along the suture zone

Integrated provenance results demonstrate that the first occurrence of Asian-derived detritus is recorded within the Denggang formation of Tethyan Himalayan strata in the study area. The continuity of the strata is a crucial basis for determining the timing of continental collision. Despite the difficulty in directly observing the contact relationship between the Denggang formation and the underlying Chuangde formation, the following evidence indicates that it was deposited above the northern Tethyan Himalaya. Firstly, the studied section is located within the area of the Tethyan Himalaya strata, approximately 10 km from the nearest suture zone deposits. Second, the Denggang formation in the studied section, which is dominated by mudstone, shows no significant deformation or metamorphism. In contrast, the Denggang formation exposed in the southern subzone of the suture zone exhibits pronounced schistosity or is incorporated into faults as displaced blocks (Xu et al., 2015). Thirdly, pink limestone blocks are also exposed in the underlying strata of the Denggang formation, consistent with observations from another section in study region and Tethyan Himalaya in central YZSZ (Fig. 8; Du et al., 2015). These suggest that the stratigraphy in the study section is continuous and the Denggang formation was deposited in the northern part of the Tethyan Himalaya.

There is significant controversy surrounding the suturing history of the Neo-Tethys in the western YZSZ. One viewpoint holds that the western YZSZ experienced multi-stage collision (e.g., Cheng et al., 2024). The appearance of Cathaysian warm-water faunas occurred in the Zhongba unit markedly earlier than in the Tethyan Himalaya, indicating that the Zhongba unit had rifted from the Indian plate during Early Permian (Cheng et al., 2022). In the central YZSZ, sedimentary evidence and mid-ocean ridge reconstructions indicate that the ophiolites originated near the southern margin of the Lhasa terrane (Dai et al., 2015; Huang et al., 2015; Gibbons et al., 2015). However, in the southern subzone of the western YZSZ, Ma et al. (2024) reported Early Cretaceous paleomagnetic data from the Xiugugabu ophiolite at 13.4°S. These data significantly differ from those of the contemporaneous Sangsang ophiolites (16°N) in the central YZSZ, but are similar to those of the Kohistan-Ladakh arc (Huang et al., 2015; Bian et al., 2023; Cao et al., 2023). The newly discovered 90 Ma arc-related magma record

within the Zhongba unit is considered to be associated with a new subduction zone in the Neo-Tethys Ocean (Cheng et al., 2024, and references therein). The above results suggest that the southern subzone may represent another subduction zone, located away from the southern margin of the Lhasa terrane. Another hypothesis posits that the western part of YZSZ underwent a single-stage India-Asia collision. One of the reasons is that melange in the two subzones share similar formation ages and the southern subzone exhibits southward kinematic features (Gansser, 1983; Xu et al., 2015; Zhou et al., 2025). Furthermore, the two subzones are closely adjacent to each other and the typical trench-arc system is only developed along the northern subzone, while the southern zone retains only the pelagic sediments and ophiolites, lacking tectonic units such as forearc basin.

In the western segment of the YZSZ, there remains insufficient research on the subduction-accretion processes of the two subzones and their collision with the Zhongba unit. Regardless of collision order, the intercontinental collision had already occurred by the time detrital materials of one continent first appeared within the other. Here, we use the initial appearance of Asian detrital material at the northern margin of the Indian plate as a benchmark to delineate the closure process of the India-Asia continental collision (Ding et al., 2017).

In the Naju area, from the Weimei Formation upward, the Denggang formation is the first strata with Asian provenance. Since the trench in middle segment of the YZSZ contains axial sediment transport pathways, constraining the initial collision timing in the western segment must also account for the potential axial delivery of Asian-derived detritus (Laskowski et al., 2019; Orme et al., 2021; Guo et al., 2022). The presence of abundant siliceous and metamorphic lithics in the Denggang formation suggests that the western Gangdese arc or oceanic crust may have experienced uplift and obduction. In the western YZSZ, the consistent provenance between the Paleogene foreland basin and the Tso-jiangding group indicates that the previously existing separation between the trench and the forearc basin had disappeared (Fig. 8; Metcalf and Kapp, 2017). The Denggang formation is predominantly composed of mudstone and siltstone, suggesting a relatively weak hydrodynamic condition. Taking these factors into account, we propose that the provenance of Denggang formation was derived from the low-relief topography of the western Gangdese arc and the Xigaze forearc basin in the western YZSZ (Liu et al., 2024). The MDAs of Denggang formation propose that initial collision occurred no later than 56 Ma - 54 Ma. This result is further supported by the timing of nappe obduction in the southern subzone and the activation of the shear zone in the Zhongba unit (Xu et al., 2015; Zhang et al., 2017). The deposition of the Denggang formation represents the direct collision of the India-Asia, rather than a continental-microcontinent collision.

In the central YZSZ, the Sangdanlin formation in the Saga area documents provenance contributions from both sides of the suture zone. Combined with tuff zircon and low-temperature thermochronology results, this constrains the initial collision time at 65 Ma to 62 Ma (Ding et al., 2005; An et al., 2021). Although the Zongzhuo formation in the Gyangze area lacks precise tuff dating results, the olistostromes and the youngest Asian block constrain the initial collision to approximately 65 Ma (Guo et al., 2024). In the eastern YZSZ, marbles and meta-siliciclastic intercalations within the Langxian unit record bilateral provenance at 56 Ma (Wei et al., 2020a, 2020b), consistent with findings from the western YZSZ. In the Nanga Parbat region, even though there's debate about the closure pattern of the Neo-Tethys, the arrival of Asian-derived material at the northern edge of the Tethyan Himalaya is constrained to 55 Ma - 50 Ma (Ding et al., 2016; Najman et al., 2017; Bhattacharya et al., 2021), aligning with the bilateral provenance time (56 Ma - 50 Ma) in the Namche Barwa region (Baral et al., 2019). The determination of the initial collision age along the suture zone rules out the continental contact first occurring in the southwestern part of the suture zone, but still remains focused in the central YZSZ (Saga to Gyangze region) (Wu et al., 2023, Fig. 9).

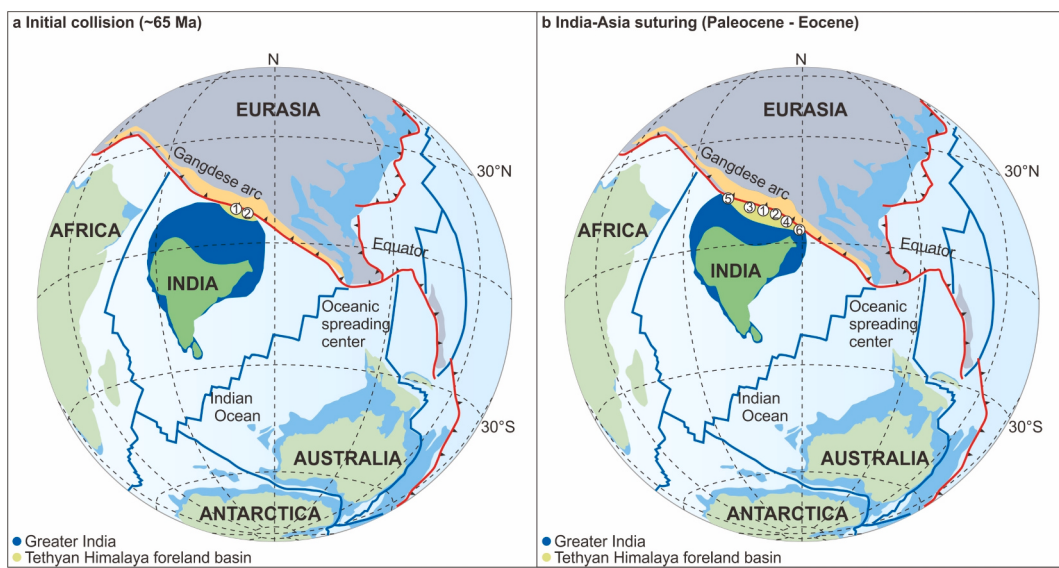


Fig. 9. The history of India–Asia suturing (modified after Ding et al., 2022). 1. Saga area, 65 Ma - 62 Ma (Ding et al., 2005; An et al., 2021); 2. Gyangze area, 65 Ma (Cai et al., 2011; Guo et al., 2024); 3. Naju section (this study), 56 Ma - 54 Ma; 4. Eastern YSZS, 60 Ma - 56 Ma (Wei et al., 2020a, 2020b); 5. Western Himalayan syntaxis: 55 Ma - 50 Ma (Ding et al., 2016; Najman et al., 2017; Bhattacharya et al., 2021); 6. Eastern Himalayan syntaxis: 56 Ma - 50 Ma (Baral et al., 2019).

7. Conclusion

In this study, we integrated field observations, detrital zircon U–Pb geochronology, trace element analyses, and machine learning to reconstruct the depositional environment, provenance, and depositional age of strata in the northern Tethyan Himalaya.

Field observations show that the northern Tethyan Himalaya strata consist of the Weimei formation, Rilang formation, Chuangde formation, and Denggang formation from bottom to top. Provenance analysis shows that the Weimei and Rilang formations exhibit typical Tethyan Himalaya characteristics, while the Denggang formation displays Asian features, indicating a shift in provenance in the northern Tethyan Himalaya. The MDAs constrain the Denggang formation to 56 Ma to 54 Ma, and this sedimentary age represents a direct collision event between the Indian and Asian continents. Our findings further support that the initial collision first occurred in the central segment of the YSZS and then temporally spread to the flanks.

Supplementary data to this article can be found online at <https://doi.org/10.1016/j.palaeo.2025.113230>.

CRediT authorship contribution statement

Xu-dong Guo: Writing – original draft. **Lin Ding:** Resources, Funding acquisition. **Fu-long Cai:** Resources, Investigation. **Gui-zhen Guo:** Resources, Formal analysis. **Xiao-yan Xu:** Software. **Peng Han:** Software, Methodology. **Chang-jun Gu:** Software. **Mei-yu Liu:** Resources. **Xiang-li Ding:** Resources, Data curation. **Xu Liu:** Methodology. **Xin-lei Li:** Software. **Deng Zeng:** Investigation. **Ya-hui Yue:** Software, Methodology. **Qiu-yun Guan:** Writing – original draft, Software, Methodology.

Declaration of competing interest

The authors declare that they have no known competing financial interests or personal relationships that could have appeared to influence the work reported in this paper.

Acknowledgments

This work benefited from financial supports from National Natural Science Foundation of China BSCTPES project (No. 41988101), Second

Tibetan Plateau Scientific Expedition and Research Program (Grant No. 2019QZKK0708) and National Natural Science Foundation of China (No. 41972239; No. 41941016; No. 42271089).

Data availability

All the data used in this study are provided in the supplementary files.

References

- Aitchison, J.C., Ali, J.R., Davis, A.M., 2007. When and where did India and Asia collide? *J. Geophys. Res. Solid Earth* 112 (B5). <https://doi.org/10.1029/2006JB004706>.
- An, W., Hu, X., Garzanti, E., 2017. Sandstone provenance and tectonic evolution of the Xiukang Mélange from Neotethyan subduction to India–Asia collision [J]. *Gondwana Res.* 41, 222–234. <https://doi.org/10.1016/j.gr.2015.08.010>.
- An, W., Hu, X., Garzanti, E., et al., 2021. New precise dating of the India-Asia collision in the Tibetan Himalaya at 61 Ma. *Geophys. Res. Lett.* 48 (3), e2020GL090641. <https://doi.org/10.1029/2020GL090641>.
- Antolín, Tomas B., 2010. Tectonic Evolution of the Tethyan Himalaya in SE Tibet Deduced from Magnetic Fabric, Structural, Metamorphic and Paleomagnetic Data [D]. Universität Tübingen.
- Baral, U., Lin, D., Goswami, T.K., et al., 2019. Detrital zircon U–Pb geochronology of a Cenozoic foreland basin in Northeast India: Implications for zircon provenance during the collision of the Indian and Asian plates[J]. *Terra Nova* 31 (1), 18–27. <https://doi.org/10.1111/ter.12364>.
- Bhattacharya, G., Robinson, D.M., Wielicki, M.M., 2021. Detrital zircon provenance of the Indus Group, Ladakh, NW India: Implications for the timing of the India-Asia collision and other syn-orogenic processes. *GSA Bull.* 133 (5–6), 1007–1020. <https://doi.org/10.1130/B35624.1>.
- Bian, W., Wang, S., Yao, Y., et al., 2023. Location and shape of the Lhasa terrane prior to India-Asia collision. *Bulletin* 135 (9–10), 2255–2274. <https://doi.org/10.1130/B36647.1>.
- Buckman, S., Aitchison, J.C., Nutman, A.P., et al., 2018. The Spongtag Massif in Ladakh, NW Himalaya: An early cretaceous record of spontaneous, intra-oceanic subduction initiation in the Neotethys. *Gondwana Res.* 63, 226–249. <https://doi.org/10.1016/j.gr.2018.07.003>.
- Cai, F., Ding, L., Yue, Y., 2011. Provenance analysis of upper Cretaceous strata in the Tethys Himalaya, southern Tibet: implications for timing of India-Asia collision[J]. *Earth Planet. Sci. Lett.* 305 (1–2), 195–206. <https://doi.org/10.1016/j.epsl.2011.02.055>.
- Cai, F., Ding, L., Leary, R.J., et al., 2012. Tectonostratigraphy and provenance of an accretionary complex within the Yarlung-Zangpo suture zone, southern Tibet: Insights into subduction-accretion processes in the Neo-Tethys[J]. *Tectonophysics* 574, 181–192. <https://doi.org/10.1016/j.tecto.2012.08.016>.
- Cai, F., Ding, L., Laskoski, A.K., et al., 2016. Late Triassic paleogeographic reconstruction along the Neo-Tethyan Ocean margins, southern Tibet. *Earth Planet. Sci. Lett.* 435, 105–114.

- Cao, Y., Sun, Z., Li, H., et al., 2023. Paleomagnetism and geochronology of early cretaceous volcanic rocks in the eastern segment of the Lhasa terrane, Tibetan Plateau, and their tectonic implications. *Bulletin* 135 (11–12), 3228–3240. <https://doi.org/10.1130/B36648.1>.
- Chen, B., Ding, L., Xu, Q., et al., 2016. U-Pb age framework of the Linzizong volcanic rocks from the Linzhou Basin, Tibet[J] (in Chinese with English abstract). *Quaternary Sciences* 36 (5), 1037–1054. <https://doi.org/10.11928/j.issn.1001-7410.2016.05.03>.
- Chen, X., Wang, C., Kuhnt, W., et al., 2011. Lithofacies, microfacies and depositional environments of Upper cretaceous Oceanic red beds (Chuangde Formation) in southern Tibet. *Sediment. Geol.* 235 (1–2), 100–110. <https://doi.org/10.1016/j.sedgeo.2010.06.008>.
- Cheng, C., Zheng, H., Kapsiotis, A., et al., 2018. Geochemistry and geochronology of dolerite dykes from the Daba and Dongbo peridotite massifs, SW Tibet: Insights into the style of mantle melting at the onset of Neo-Tethyan subduction. *Lithos* 322, 281–295. <https://doi.org/10.1016/j.lithos.2018.10.023>.
- Cheng, J.B., Li, Y.L., Li, S., et al., 2022. Reconstruction of the South Qiangtang–Zhongba–Tethyan Himalaya continental margin system along the northern Indian Plate: Insights from the paleobiogeography of the Zhongba microterrane. *J. Asian Earth Sci.* 240, 105376. <https://doi.org/10.1016/j.jseas.2022.105376>.
- Cheng, J.B., Li, Y.L., Li, X., et al., 2024. Radiolarian-based stratigraphic reconstruction along the western Yarlung–Tsangpo suture zone, southern Tibet, and its implication for Neo-Tethyan late-stage evolution. *Geol. Soc. Am. Bull.* <https://doi.org/10.1130/B37557.1>.
- Colpaert, C.P.A.M., Li, G., 2021. Uppermost Jurassic to lower cretaceous benthic foraminiferal faunas of the Weimei and the Bandingsi localities of northern and southern parts of South Tibet—a preliminary analysis. *Cretac. Res.* 124, 104785. <https://doi.org/10.1016/j.cretres.2021.104785>.
- Cui, X., Luo, H., Aitchison, J.C., et al., 2021. Middle Jurassic radiolarians and chert geochemistry, Dajiweng ophiolite, SW Tibet: Implications for Neotethyan Ocean evolution. *J. Asian Earth Sci.* 221, 104947. <https://doi.org/10.1016/j.jseas.2021.104947>.
- Dai, J., Wang, C., Li, Y., 2012. Relicts of the early cretaceous seamounts in the central-western Yarlung Zangbo Suture Zone, southern Tibet. *J. Asian Earth Sci.* 53, 25–37. <https://doi.org/10.1016/j.jseas.2011.12.024>.
- Dai, J., Wang, C., Zhu, D., et al., 2015. Multi-stage volcanic activities and geodynamic evolution of the Lhasa terrane during the cretaceous: Insights from the Xigaze forearc basin. *Lithos* 218, 127–140. <https://doi.org/10.1016/j.lithos.2015.01.019>.
- DeCelles, P.G., Kapp, P., Gehrels, G.E., et al., 2014. Paleocene–Eocene foreland basin evolution in the Himalaya of southern Tibet and Nepal: Implications for the age of initial India–Asia collision. *Tectonics* 33 (5), 824–849. <https://doi.org/10.1002/2014TC003522>.
- Dickinson, W.R., 1985. *Interpreting Provenance Relations from Detrital Modes of Sandstones*. Springer, Netherlands, pp. 333–361.
- Dickinson, W.R., Gehrels, G.E., 2009. Use of U-Pb ages of detrital zircons to infer maximum depositional ages of strata: A test against a Colorado Plateau Mesozoic database[J]. *Earth Planet. Sci. Lett.* 288 (1–2), 115–125. <https://doi.org/10.1016/j.epsl.2009.09.013>.
- Ding, L., Kapp, P., Wan, X., 2005. Paleocene–Eocene record of ophiolite obduction and initial India–Asia collision, south central Tibet[J]. *Tectonics* 24 (3). <https://doi.org/10.1029/2004TC001729>.
- Ding, L., Qasim, M., Jadoon, I.A.K., et al., 2016. The India–Asia collision in north Pakistan: Insight from the U-Pb detrital zircon provenance of Cenozoic foreland basin[J]. *Earth Planet. Sci. Lett.* 455, 49–61. <https://doi.org/10.1016/j.epsl.2016.09.003>.
- Ding, L., Maksatbek, S., Cai, F.L., et al., 2017. Processes of initial collision and suturing between India and Asia. *Sci. China Earth Sci.* 60, 635–651. <https://doi.org/10.1007/s11430-016-5244-x>.
- Ding, L., Kapp, P., Cai, F., et al., 2022. Timing and mechanisms of Tibetan Plateau uplift. *Nat. Rev. Earth Environ.* 3 (10), 652–667. <https://doi.org/10.1038/s43017-022-00318-4>.
- Du, X., Chen, X., Wang, C., et al., 2015. Geochemistry and detrital zircon U-Pb dating of Lower Cretaceous volcanoclastics in the Babazhadong section, Northern Tethyan Himalaya: Implications for the breakup of Eastern Gondwana[J]. *Cretac. Res.* 52, 127–137. <https://doi.org/10.1016/j.cretres.2014.08.002>.
- Fang, P., Xu, B., Huber, B.T., et al., 2020. Late Campanian to early Maastrichtian planktonic foraminiferal assemblages from cretaceous oceanic red beds (CORBs) in the Yongla section, Gyangze, southern Tibet. *Micropaleontology* 66 (2). <https://doi.org/10.47894/mpal.66.2.01>.
- Gansser, A., 1983. *The Wider Himalaya, a Model for Scientific Research*[M]. Munksgaard, Kommissionär.
- Gibbons, A.D., Zahirovic, S., Müller, R.D., et al., 2015. A tectonic model reconciling evidence for the collisions between India, Eurasia and intra-oceanic arcs of the central-eastern Tethys. *Gondwana Res.* 28 (2), 451–492. <https://doi.org/10.1016/j.gr.2015.01.001>.
- Grimes, C.B., Wooden, J.L., Cheadle, M.J., John, B.E., 2015. “Fingerprinting” tectonomagnetic provenance using trace elements in igneous zircon. *Contrib. Mineral. Petro.* 170 (5), 1–26. <https://doi.org/10.1007/s00410-015-1199-3>.
- Guo, X., Ding, L., Cai, F., et al., 2019. Subduction and accretion process of the western segment of the Yarlung Zangbo suture zone in Zhongba area, Tibet[J] (in Chinese with English abstract). *Chin. J. Geol.* 54 (4), 1031–1047. <https://doi.org/10.12017/dzgx.2019.058>.
- Guo, X., Ding, L., Laskowski, A.K., et al., 2022. Provenance of Late Cretaceous accretionary complex within the Yarlung–Zangpo suture zone, Bainang, southern Tibet: Implications for the subduction–accretion of the Neo-Tethyan ocean[J]. *Gondwana Res.* 106, 78–91. <https://doi.org/10.1016/j.gr.2022.01.004>.
- Guo, X., Ding, L., Guan, Q., et al., 2024. Timing of India–Asia suturing: evidence from a remnant peripheral foreland basin in Xigaze, South Tibet. *Palaeogeogr. Palaeoclimatol. Palaeoecol.* 638, 112043. <https://doi.org/10.1016/j.palaeo.2024.112043>.
- He, J., Li, Y., Hou, Y., et al., 2024. Early Triassic Volcanic Rocks in the Western Yarlung Zangbo Suture Zone: Implications for the opening of the Neo-Tethys Ocean. *Acta Geologica Sinica - English Edition* 98, 324–336. <https://doi.org/10.1111/1755-6724.15141>.
- Hebei Institute of Geological Survey, 2006. *Reports on the 1:250 000 Regional Geological Survey—Yagra, Burang, Horba and Babazhadong Sheets in Xizang*. China Geological Survey, Beijing, 307 p. (in Chinese).
- Hu, X., Jansa, L., Chen, L., et al., 2010. Provenance of lower cretaceous Wölong Volcanoclastics in the Tibetan Tethyan Himalaya: Implications for the final breakup of Eastern Gondwana. *Sediment. Geol.* 223 (3), 193–205. <https://doi.org/10.1016/j.sedgeo.2009.11.008>.
- Hu, X., Garzanti, E., Moore, T., et al., 2015. Direct stratigraphic dating of India–Asia collision onset at the Selandian (middle Paleocene, 59±1 Ma). *Geology* 43 (10), 859–862. <https://doi.org/10.1130/G36872.1>.
- Hu, X., Wang, J., BouDagher-Fadel, M., et al., 2016. New insights into the timing of the India–Asia collision from the Paleogene Quxia and Jialazi formations of the Xigaze forearc basin, South Tibet[J]. *Gondwana Res.* 32, 76–92. <https://doi.org/10.1016/j.gr.2015.02.007>.
- Huang, W., van Hinsbergen, D.J.J., Maffione, M., et al., 2015. Lower cretaceous Xigaze ophiolites formed in the Gangdese forearc: evidence from paleomagnetism, sediment provenance, and stratigraphy. *Earth Planet. Sci. Lett.* 415, 142–153. <https://doi.org/10.1016/j.epsl.2015.01.032>.
- Jackson, S.E., Pearson, N.J., Griffin, W.L., Belousova, E.A., 2004. The application of laser ablation-inductively coupled plasma-mass spectrometry to in situ U-Pb zircon geochronology. *Chem. Geol.* 211 (1), 47–69. <https://doi.org/10.1016/j.chemgeo.2004.06.017>.
- Ji, W.Q., Wu, F.Y., Chung, S.L., et al., 2009. Zircon U-Pb geochronology and Hf isotopic constraints on petrogenesis of the Gangdese batholith, southern Tibet[J]. *Chem. Geol.* 262 (3–4), 229–245. <https://doi.org/10.1016/j.chemgeo.2009.01.020>.
- Jiang, J., Zheng, Y., Gao, S., et al., 2018. The newly-discovered late cretaceous igneous rocks in the Nuocang district: Products of ancient crust melting triggered by Neo-Tethyan slab rollback in the western Gangdese. *Lithos* 308–309, 294–315. <https://doi.org/10.1016/j.lithos.2018.03.009>.
- Jin, S.C., Tong, Y.B., Sun, X.X., et al., 2024. Extensional tectonics of the Indian passive continental margin in the Middle and late Jurassic: Constraints from detrital zircon ages in the eastern Tethyan Himalaya. *J. Geodyn.* 159, 102019.
- Kapp, P., DeCelles, P.G., 2019. Mesozoic–Cenozoic geological evolution of the Himalayan–Tibetan orogen and working tectonic hypotheses. *Am. J. Sci.* 319 (3), 159–254. <https://doi.org/10.2475/03.2019.01>.
- Laskowski, A.K., Kapp, P., Ding, L., et al., 2017. Tectonic evolution of the Yarlung suture zone, Lopu Range region, southern Tibet. *Tectonics* 36 (1), 108–136. <https://doi.org/10.1029/2016TC004334>.
- Laskowski, A.K., Orme, D.A., Cai, F., Ding, L., 2019. The Ancestral Lhasa River: a late cretaceous trans-arc river that drained the proto-Tibetan Plateau. *Geology* 47 (11), 1029–1033. <https://doi.org/10.1130/g46823.1>.
- Li, G., Jiang, G., Wan, X., 2011. The age of the Chuangde Formation in Kangmar, southern Tibet of China: Implications for the origin of cretaceous oceanic red beds (CORBs) in the northern Tethyan Himalaya. *Sediment. Geol.* 235 (1–2), 111–121. <https://doi.org/10.1016/j.sedgeo.2010.04.011>.
- Li, G., Holbourn, A., Kuhnt, W., et al., 2020a. Occurrence of benthic foraminifers across the Jurassic/cretaceous transition in Gyangze, southern Xizang (Tibet), China. *Cretac. Res.* 105, 103931. <https://doi.org/10.1016/j.cretres.2018.08.001>.
- Li, S., Ding, L., Fu, J.J., Yue, Y.H., 2016. Age, provenance and tectonic setting of Dajin conglomerate, Tibet[J] (in Chinese with English abstract). *Acta Petrol. Sin.* 32 (11), 3537–3546.
- Li, S., Wei, M., Huang, T., et al., 2023a. Zircon U-Pb geochronology of the Gongzhu Conglomerate in the Zhongba block from Ali, Tibet and its geological significance[J] (in Chinese with English abstract). *Bull. Geol. Sci. Technol.* 42 (1), 191–203.
- Li, S., Li, Y., Tan, X., et al., 2024. Early–Middle Devonian paleomagnetic results from the Zhongba microterrane, Tibetan Plateau: evidence for its origin from the northern margin of Greater India. *Geol. Soc. Am. Bull.* <https://doi.org/10.1130/B37147.1>.
- Li, X., Wang, C., Li, Y., et al., 2014. Definition and composition of the Zhongba Microterrane in Southwest Tibet[J] (in Chinese with English abstract). *Acta Geol. Sin.* 88 (8), 1372–1381. <https://doi.org/10.19762/j.cnki.dizhixuebao.2014.08.002>.
- Li, X., Li, Y., Wang, C., et al., 2018. Paleocene Radiolarian Faunas in the Deep-Marine Sediments near Zhongba County, southern Tibet. *Paleontol. Res.* 22 (1), 37–56. <https://doi.org/10.2517/2017PR009>.
- Li, X., Matsuoka, A., Bertinelli, A., et al., 2020b. Correlation of early cretaceous radiolarian assemblages from southern Tibet and Central Italy. *Cretac. Res.* 105, 104046. <https://doi.org/10.1016/j.cretres.2018.12.016>.
- Li, X., Suzuki, N., Meng, J., et al., 2023b. Constraints on the expanse of Greater India in the early cretaceous from radiolarians. *Earth Planet. Sci. Lett.* 622, 118413.
- Li, X., Hu, X.M., An, W., et al., 2023c. From Neo-Tethyan convergence to India–Asia collision: radiolarian biostratigraphy of the cretaceous to Paleocene deep-water Tethys Himalaya. *Newsl. Stratigr.* 56 (1), 33–52. <https://doi.org/10.1127/nos/2022/0707>.
- Liang, Y., Zhang, K., Xu, Y., et al., 2012. Late Paleocene radiolarian fauna from Tibet and its geological implications. *Can. J. Earth Sci.* 49 (11), 1364–1371. <https://doi.org/10.1139/e2012-054>.

- Liu, F., Dilek, Y., Xie, Y., et al., 2018. Melt evolution of upper mantle peridotites and mafic dikes in the northern ophiolite belt of the western Yarlung Zangbo suture zone (southern Tibet). *Lithosphere* 10 (1), 109–132. <https://doi.org/10.1130/L689.1>.
- Liu, F., Dilek, Y., Yang, J.S., et al., 2021. A middle Triassic seamount within the western Yarlung Zangbo suture zone, Tibet: the earliest seafloor spreading record of Neotethys to the North of East Gondwana. *Lithos* 388, 106062. <https://doi.org/10.1016/j.lithos.2021.106062>.
- Liu, X., Tang, M., Cao, W., et al., 2024. Sluggish rise of the western Gangdese mountains after India-Eurasia collision. *Lithos* 478, 107640. <https://doi.org/10.1016/j.lithos.2024.107640>.
- Liu, Y., Ji, Q., Jiang, X., et al., 2013. U-Pb zircon ages of early cretaceous volcanic rocks in the Tethyan Himalaya at Yangzuoong Co lake, Nagarze, Southern Tibet, and implications for the Jurassic/Cretaceous boundary[J]. *Cretac. Res.* 40, 90–101. <https://doi.org/10.1016/j.cretres.2012.05.010>.
- Ma, L., Wang, Q., Tang, G.J., Li, C., 2022. Nature and evolution of crust in the southern Lhasa during Phanerozoic[J] (in chinese with English abstract). *Geotecton. Metallog.* 46 (06), 1170–1184.
- Ma, X., Tan, X., Li, Y., et al., 2024. Paleolatitude of Mafic Dykes in the Xiugugabu ophiolite: Implications for the intraoceanic Trans-Tethyan subduction zone and multistage India-Eurasia collision. *Tectonophysics*, 230466. <https://doi.org/10.1016/j.tecto.2024.230466>.
- Meng, J., Gilder, S., Tan, X., et al., 2023. Strengthening the argument for a large Greater India. *Proc. Natl. Acad. Sci.* 120 (33), e2305928120. <https://doi.org/10.1073/pnas.2305928120>.
- Metcalf, K., Kapp, P., 2017. The Yarlung suture Mélange, Lopu Range, southern Tibet: Provenance of sandstone blocks and transition from oceanic subduction to continental collision. *Gondwana Res.* 48, 15–33. <https://doi.org/10.1016/j.gr.2017.03.002>.
- Murphy, M., Yin, A., 2003. Structural evolution and sequence of thrusting in the Tethyan fold-thrust belt and Indus-Yalu suture zone, Southwest Tibet. *Geol. Soc. Am. Bull.* 115 (1), 21–34. [https://doi.org/10.1130/0016-7606\(2003\)115<0021:SEASOT>2.0.CO;2](https://doi.org/10.1130/0016-7606(2003)115<0021:SEASOT>2.0.CO;2).
- Najman, Y., Jenks, D., Godin, L., et al., 2017. The Tethyan Himalayan detrital record shows that India-Asia terminal collision occurred by 54 Ma in the Western Himalaya [J]. *Earth Planet. Sci. Lett.* 459, 301–310. <https://doi.org/10.1016/j.epsl.2016.11.036>.
- Orme, D.A., Carrapa, B., Kapp, P., 2015. Sedimentology, provenance and geochronology of the upper Cretaceous-lower Eocene western Xigaze forearc basin, southern Tibet. *Basin Res.* 27 (4), 387–411. <https://doi.org/10.1111/bre.12080>.
- Orme, D.A., Laskowski, A.K., Zilinsky, M.F., et al., 2021. Sedimentology and provenance of newly identified Upper Cretaceous trench basin strata, Dênggar, southern Tibet: Implications for development of the Eurasian margin prior to India-Asia collision. *Basin Res.* 33 (2), 1454–1473.
- Sun, G., Hu, X., 2012. Tectonic affinity of Zhongba terrane: Evidences from the detrital zircon geochronology and Hf isotopes[J] (in Chinese with English abstract). *Acta Petrol. Sin.* 28 (5), 1635–1646.
- Sun, G., Wang, J., Hu, X., et al., 2018. Upper Cretaceous-lower Eocene Dajiweng Formation in the Zhada area, southern Tibet: Implications for the Trans-Himalayan forearc basin evolution[J] (in Chinese with English abstract). *Acta Petrol. Sin.* 34 (6), 1847–1861.
- Van Hinsbergen, D.J.J., Lippert, P.C., Dupont-Nivet, G., et al., 2012. Greater India Basin hypothesis and a two-stage Cenozoic collision between India and Asia. *Proc. Natl. Acad. Sci.* 109 (20), 7659–7664. <https://doi.org/10.1073/pnas.1117262109>.
- Wang, C., Ding, L., Zhang, L.Y., et al., 2016. Petrogenesis of Middle-Late Triassic volcanic rocks from the Gangdese belt, southern Lhasa terrane: Implications for early subduction of Neo-Tethyan oceanic lithosphere. *Lithos* 262, 320–333. <https://doi.org/10.1016/j.lithos.2016.07.021>.
- Wang, C., Ding, L., Liu, Z., et al., 2017a. Early cretaceous bimodal volcanic rocks in the southern Lhasa terrane, South Tibet: Age, petrogenesis and tectonic implications. *Lithos* 268–271, 260–273. <https://doi.org/10.1016/j.lithos.2016.11.016>.
- Wang, H., Ding, L., Cai, F., et al., 2017b. Early tertiary deformation of the Zhongba-Gyangze thrust in central southern Tibet[J]. *Gondwana Res.* 41, 235–248. <https://doi.org/10.1016/j.gr.2015.02.017>.
- Wang, J., Hu, X., Jansa, L., et al., 2011. Provenance of the Upper Cretaceous–Eocene deep-water sandstones in Sangdanlin, southern Tibet: Constraints on the timing of initial India-Asia collision[J]. *J. Geol.* 119 (3), 293–309. <https://doi.org/10.1086/659145>.
- Wang, J.G., Hu, X.M., BouDagher-Fadel, M., et al., 2015. Early Eocene sedimentary recycling in the Kailas area, southwestern Tibet: Implications for the initial India-Asia collision[J]. *Sediment. Geol.* 315, 1–13. <https://doi.org/10.1016/j.sedgeo.2014.10.009>.
- Wang, T., Li, G., Elmes, M., 2021. Biostratigraphy and provenance analysis of the cretaceous to Palaeogene deposits in southern Tibet: Implications for the India-Asia collision. *Basin Res.* 33 (3), 1749–1775. <https://doi.org/10.1111/bre.12534>.
- Wei, Y., Li, Y., Chen, X., Zhong, H.T., et al., 2015. The reconstruction of oceanic plate stratigraphy and its implications: a case study of Zhongba area, southern Tibet[J] (in Chinese with English abstract). *Geol. Bull. China* 34 (10), 1789–1801.
- Wei, Y., Liang, W., Shang, Y., et al., 2017. Petrogenesis and tectonic implications of ~ 130 Ma diabase dikes in the western Tethyan Himalaya (western Tibet). *J. Asian Earth Sci.* 143, 236–248. <https://doi.org/10.1016/j.jseas.2017.04.008>.
- Wei, Z., Li, X., Li, Y., et al., 2020a. Discovery of Vestige Sedimentary Archives of the India-Asia Collision in the Eastern Yarlung Zangbo Suture Zone. *J. Geophys. Res. Solid Earth* 125 (4), e2019JB018192. <https://doi.org/10.1029/2019JB018192>.
- Wei, Z., Li, X., Sinclair, H., et al., 2020b. The embryonic Himalayan foreland basin revealed in the eastern Yarlung Zangbo suture zone, southeastern Tibet. *Sediment. Geol.* 407, 105743. <https://doi.org/10.1016/j.sedgeo.2020.105743>.
- Wu, F., Ji, W., Wang, J., et al., 2014. Zircon U-Pb and Hf isotopic constraints on the onset time of India-Asia collision[J]. *Am. J. Sci.* 314 (2), 548–579. <https://doi.org/10.2475/02.2014.04>.
- Wu, F.Y., Ji, W.Q., Liu, C.Z., et al., 2010. Detrital zircon U-Pb and Hf isotopic data from the Xigaze fore-arc basin: Constraints on Transhimalayan magmatic evolution in southern Tibet[J]. *Chem. Geol.* 271 (1–2), 13–25. <https://doi.org/10.1016/j.chemgeo.2009.12.007>.
- Wiedenbeck, M., Alle, P., Corfu, F., Griffin, W.L., Meier, M., Oberli, F., Quadri, A.V., Roddick, J.C., Spiegel, W., 1995. Three natural zircon standards for U-Th-Pb, Lu-Hf, trace element and REE analyses. *Geostand. Newsltt.* 19 (1), 1–23.
- Wu, X., Hu, J., Chen, L., et al., 2023. Paleogene India-Eurasia collision constrained by observed plate rotation. *Nat. Commun.* 14 (1), 7272. <https://doi.org/10.1038/s41467-023-42920-0>.
- Xiong, F., Meng, Y., Yang, J., et al., 2020. Geochronology and petrogenesis of the mafic dykes from the Purang ophiolite: Implications for evolution of the western Yarlung-Tsango suture zone, southwestern Tibet. *Geosci. Front.* 11 (1), 277–292. <https://doi.org/10.1016/j.gsf.2019.05.006>.
- Xu, Z., Dilek, Y., Yang, J., et al., 2015. Crustal structure of the Indus-Tsangpo suture zone and its ophiolites in southern Tibet[J]. *Gondwana Res.* 27 (2), 507–524. <https://doi.org/10.1016/j.gr.2014.08.001>.
- Yang, S., Liang, X., Jiang, M., et al., 2022. Slab remnants beneath the Myanmar terrane evidencing double subduction of the Neo-Tethyan Ocean. *Sci. Adv.* 8 (34), eab0127. <https://doi.org/10.1126/sciadv.ab0127>.
- Yin, A., Harrison, T.M., 2000. Geologic evolution of the Himalayan-Tibetan orogen. *Annu. Rev. Earth Planet. Sci.* 28 (1), 211–280. <https://doi.org/10.1146/annurev.earth.28.1.211>.
- Yuan, J., Yang, Z., Deng, C., et al., 2021. Rapid drift of the Tethyan Himalaya terrane before two-stage India-Asia collision. *Natl. Sci. Rev.* 8 (7), nwaa173. <https://doi.org/10.1093/nsr/nwaa173>.
- Yuan, J., Deng, C., Yang, Z., et al., 2023. New paleomagnetic data from the central Tethyan Himalaya refine the size of Greater India during the Campanian. *Earth Planet. Sci. Lett.* 622, 118422. <https://doi.org/10.1016/j.epsl.2023.118422>.
- Zhang, B., Liu, X.P., Li, S.Y., et al., 2017. ^{40}Ar – ^{39}Ar Ages of the ductile decollement shear zone in the Zhongba microterrane of Saga region, Southwest Tibet, and their geological significance[J] (in Chinese with English abstract). *Geol. Bull. China* 36 (6), 933–944.
- Zhang, L., Dueca, M.N., Ding, L., et al., 2014. Southern Tibetan Oligocene–Miocene adakites: A record of Indian slab tearing[J]. *Lithos* 210–211, 209–223. <https://doi.org/10.1016/j.lithos.2014.09.029>.
- Zhang, S., Mahoney, J.J., Mo, X., et al., 2005. Evidence for a Widespread Tethyan Upper Mantle with Indian-Ocean-Type Isotopic Characteristics. *J. Petrol.* 46 (4), 829–858. <https://doi.org/10.1093/petrology/egi002>.
- Zhang, X., Wei, Y., Wang, C., et al., 2015. Provenance analysis and its tectonic significance of early cretaceous Rilang Formation in Zhongba area, southern Tibet[J] (in Chinese with English abstract). *Acta Petrol. Sin.* 31 (1), 273–283.
- Zhong, S.H., Liu, Y., Li, S.Z., et al., 2023. A machine learning method for distinguishing detrital zircon provenance. *Contrib. Mineral. Petro.* 178, 35. <https://doi.org/10.1007/s00410-023-02017-9>.
- Zhou, H.F., Zhang, Y.C., Mao, L., et al., 2025. Dismembered Guadalupian (Middle Permian) seamounts within the Yarlung-Tsangpo Suture Zone: Implications for the opening time of the Neo-Tethys Ocean. *Palaeogeogr. Palaeoclimatol. Palaeoecol.* 675, 113063. <https://doi.org/10.1016/j.palaeo.2025.113063>.
- Zhu, D., Wang, Q., Zhao, Z., et al., 2015. Magmatic record of India-Asia collision. *Sci. Rep.* 5 (1), 14289. <https://doi.org/10.1038/srep17236>.
- Zhu, D.C., Zhao, Z.D., Niu, Y., et al., 2011a. The Lhasa Terrane: Record of a microcontinent and its histories of drift and growth. *Earth Planet. Sci. Lett.* 301. <https://doi.org/10.1016/j.epsl.2010.11.005>.
- Zhu, D.C., Zhao, Z.D., Niu, Y., et al., 2011b. Lhasa terrane in southern Tibet came from Australia. *Geology* 39 (8), 727–730. <https://doi.org/10.1130/G31895.1>.
- Zhu, D.C., Wang, Q., Chung, S.L., et al., 2018. Gangdese magmatism in southern Tibet and India-Asia convergence since 120 Ma. Gangdese magmatism in southern Tibet and India-Asia convergence since 120 Ma. *Geological Society, London. Spec. Publ.* 483, 583–604. <https://doi.org/10.1144/SP483.14>.
- Ziabrev, S.V., Aitchison, J.C., Abravetsch, A.V., et al., 2004. Bainang Terrane, Yarlung-Tsangpo suture, southern Tibet (Xizang, China): a record of intra-Neotethyan subduction-accretion processes preserved on the roof of the world. *J. Geol. Soc. London* 161, 523–539. <https://doi.org/10.1144/0016-764903-099>.